ADVANCED MATERIALS

[7] M. M. Baksh, M. Jaros, J. T. Groves, *Nature* **2004**, *427*, 139.
[8] A. Grakoui, S. K. Bromley, C. Sumen, M. M. Davis, A. S. Shaw, P. M. Allen, M. L. Dustin, *Science* **1999**, *285*, 221.
[9] S. Damjanovich, R. Gaspar, Jr., C. Pieri, *Q. Rev. Biophys.* **1997**, *30*, 67.
[10] J. T. Groves, *Angew. Chem. Int. Ed.*, in press.
[11] B. Jackson, J. T. Groves, *J. Am. Chem. Soc.* **2004**, *126*, 13 878.
[12] J. T. Groves, S. G. Boxer, *Acc. Chem. Res.* **2002**, *35*, 149.
[13] J. T. Groves, N. Ulman, S. G. Boxer, *Science* **1997**, *275*, 651.
[14] J. S. Hovis, S. G. Boxer, *Langmuir* **2000**, *16*, 894.
[15] J. S. Hovis, S. G. Boxer, *Langmuir* **2001**, *17*, 3400.
[16] L. Kam, S. G. Boxer, *J. Am. Chem. Soc.* **2000**, *122*, 12 901.
[17] L. Kam, S. G. Boxer, *Langmuir* **2003**, *19*, 1624.
[18] C. K. Yee, M. L. Amweg, A. N. Parikh, *Adv. Mater.* **2004**, *16*, 1184.
[19] C. K. Yee, M. L. Amweg, A. N. Parikh, *J. Am. Chem. Soc.* **2004**, *126*, 13 962.
[20] J. R. Vig, *J. Vac. Sci. Technol., A* **1985**, *3*, 1027.
[21] O. Legrini, E. Oliveros, A. M. Braun, *Chem. Rev.* **1993**, *93*, 671.
[22] P. Wentworth, Jr., L. H. Jones, A. D. Wentworth, X. Zhu, N. A. Larsen, I. A. Wilson, X. Xu, W. A. Goddard, III, K. D. Janda, A. Eschenmoser, R. A. Lerner, *Science* **2001**, *293*, 1806.
[23] P. Wentworth, Jr., L. H. Jones, A. D. Wentworth, X. Zhu, N. A. Larsen, I. A. Wilson, X. Xu, W. A. Goddard, III, K. D. Janda, A. Eschenmoser, R. A. Lerner, *Science* **2002**, *298*, 2195.
[24] P. M. Kasson, V. S. Pande, *Biophys. J.* **2004**, *86*, 3744.
[25] Y. Kaizuka, J. T. Groves, *Biophys. J.* **2004**, *86*, 905.
[26] M. A. Holden, S. Y. Jung, T. Yang, E. T. Castellana, P. S. Cremer, *J. Am. Chem. Soc.* **2004**, *126*, 6512.

Bottom–Up Fabrication of Carbon-Rich Silicon Carbide Nanowires by Manipulation of Nanometer-Sized Ethanol Menisci**

By *Marta Tello*, *Ricardo Garcia*,* *José Angel Martín-Gago*, *Nicolás F. Martínez*, *María Soledad Martín-González*, *Lucia Aballe*, *Alexis Baranov*, and *Luca Gregoratti*

The development of nanometer-scale lithographies is the focus of intense research activity because progress on nanotechnology depends on the capability to fabricate, position, and interconnect nanometer-scale structures.[1] The unique imaging and manipulation properties of atomic force microscopy (AFM) has prompted the emergence of several scanning-probe-based nanolithographies.[2–5] Here we describe an atomic force nanolithography based on the spatial confinement of an electrochemical reaction within a nanometer-sized ethanol meniscus. The meniscus is induced by the application of an electrical field. The end result is the formation of a nanometer-sized electrochemical cell (nanocell) that contains about 5×10^4 molecules. The reduced number of molecules and the reaction kinetics allows a bottom–up fabrication of several types of nanostructures. We show, using spatially resolved photoemission spectroscopy, that the nanostructures are made of carbon-rich SiC. The nanolithographic possibilities are illustrated by the fabrication of nanowires with widths and positioning below 45 nm, both singly or forming arbitrarily shaped networks.

AFM nano-oxidation[4] (local oxidation nanolithography) has allowed the fabrication of a variety of nanometer-scale devices such as 0.2 terabit cm^{-2} memories,[6,7] superconducting quantum interference devices,[8,9] or templates for driving the growth of organic molecules.[10] Parallel patterning based on local oxidation has also been demonstrated by replacing the AFM tip with a stamp with multiple lines or protrusions.[11,12] AFM local oxidation is based on the spatial confinement of the electrochemical oxidation between the tip and the sample surface.[6,13] This requires the formation and manipulation of tiny water bridges.[14,15] The directly fabricated structures are oxides of the sample surface that may serve as a tunnel barriers in nanoelectronic devices, templates, or masks for further processing.[16–20] The local oxidation process is robust, low-cost, and compatible with ambient operation. However, it is severely limited because it only generates oxides of materials that are amenable for anodic oxidation.

We have developed a method to obtain a variety of nanometer-sized carbide structures. The method is based on the ability to form and manipulate the properties of ethyl alcohol nanometer-sized bridges. The ethanol bridge is formed by the application of an electrical field between an n-doped silicon tip and a silicon surface. Once an ethanol nanocell has been formed, a voltage pulse drives the ethanol molecules to a Si(100) interface where the electrochemical reaction occurs. The experimental set-up consists of a conductive dynamic AFM which is enclosed in a chamber filled with N_2 and CH_3CH_2OH vapor. A voltage pulse applied between tip and sample condenses the vapor underneath the AFM tip, giving rise to the formation of a nanometer-sized liquid bridge. Tip–surface separation, voltage strength, and pulse duration control the meniscus size and hence the electrochemical cell's size, which in turns will control the nanostructure size.

Some elements of the experimental set-up and the steps involved in the formation of nanometer-sized liquid bridges are shown schematically in Figure 1. The instantaneous motion of the AFM tip is recorded in an oscilloscope screen. Before the application of a voltage pulse, the tip oscillates above the sample surface. The electrostatic interaction deflects the tip's

[*] Prof. R. Garcia, Dr. M. Tello, N. F. Martínez, Dr. M. S. Martín-González
Instituto de Microelectrónica de Madrid, CSIC
E-28760 Tres Cantos, Madrid (Spain)
E-mail: rgarcia@imm.cnm.csic.es
Dr. J. A. Martín-Gago
Instituto de Ciencia de Materiales de Madrid, CSIC, Campus Cantoblanco
E-28049 Madrid (Spain)
Dr. L. Aballe, Dr. A. Baranov, Dr. L. Gregoratti
ELETTRA, Sincrotrone Trieste S.c.p.a.
I-34012 Trieste (Italy)

[**] This work was supported by Ministerio de Educacion y Ciencia (Spain) contract number MAT2003-02655 and the European Commission, contract number NAIMO Integrated Project No NMP4-CT-2004-500355.

  DOI: 10.1002/adma.200401466

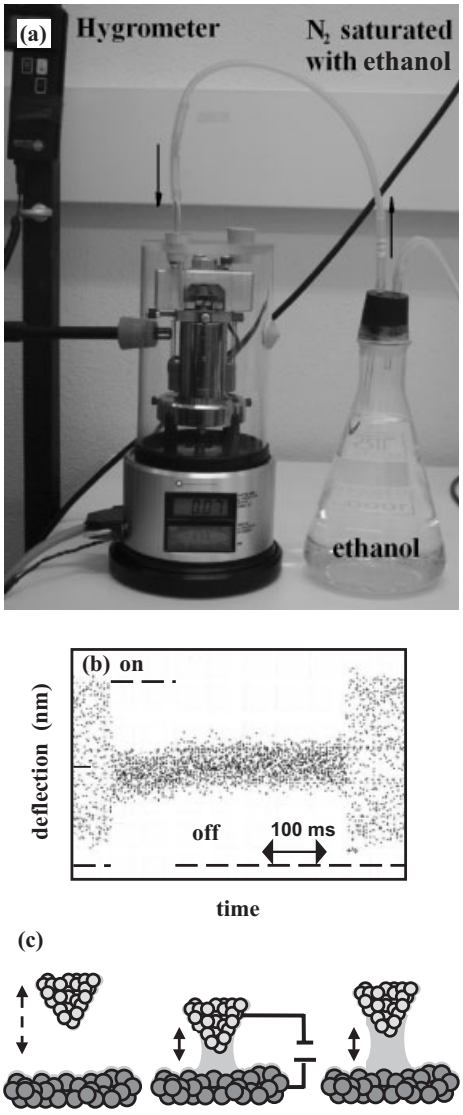

Figure 1. Experimental set-up for the formation and monitoring of nanometer-sized ethanol liquid bridges. a) AFM environmental control chamber with dry N_2 and ethanol vapor pipelines. b) Cantilever-tip oscillation (deflection) before, during, and after the application of a voltage pulse. Each dot represents the instantaneous AFM-tip amplitude. Once the pulse is off, the ethanol meniscus holds the cantilever; however, because the capillary force is smaller than electrostatic force, the cantilever moves its average position away from the surface. The dashed line represents the voltage pulse. Deflection full range is 11 nm. c) Physical interpretation of the changes in the oscillation amplitude displayed in (b). The arrows depicts the tip oscillation.

equilibrium position and changes the AFM resonant frequency which leads to a reduction of the oscillation amplitude. Once the pulse is off, the oscillation amplitude remains reduced because the capillary force of the ethanol bridge holds the tip. Finally, the tip is retracted, which causes the bridge to stretch and eventually break; the tip then recovers its initial amplitude (Fig. 1b).

When an ethanol meniscus bridges tip and sample surface, another voltage pulse is applied to initiate the electrochemical reaction. The application of a single pulse generates a dot the size of which depends on the voltage strength, pulse duration, and bridge size.[21] Figure 2a shows several dots fabricated by the application of a series of 16 V pulses for 1 s (sample positive). In this case, each dot has required the formation of a nanocell. The dot size is 30–60 nm in width and 2 nm in height. The sequential application of voltage pulses in the situation where the size of the individual nanostructure is larger than lateral distance between pulses allows the fabrication of continuous wires. A wire of 5.5 μm length and 60 nm width is shown in Figure 2b. Similarly, several nanowire structures can be fabricated such as arrays of parallel or interconnected wires.

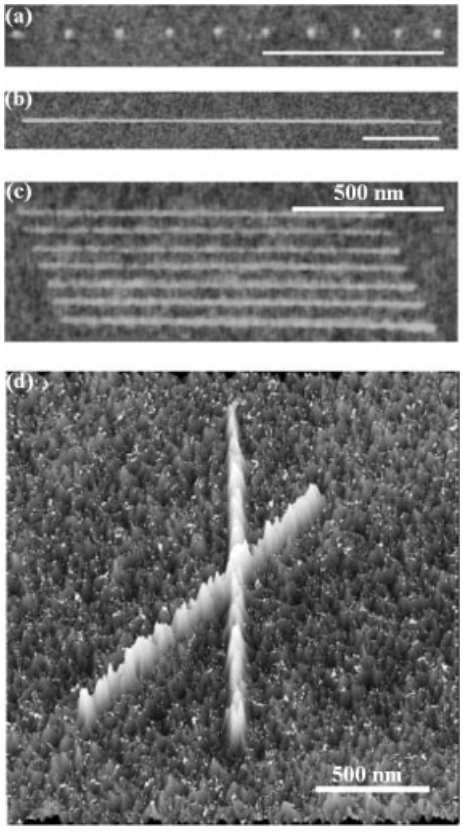

Figure 2. AFM images of nanostructures fabricated in an ethyl alcohol nanocell. a) A series of nanodots spaced 220 nm apart; width range 40–60 nm. Scale bar: 1 μm. b) A single nanowire. Scale bar: 1 μm. c) A parallel array of nanowires. The wires are placed 70 nm part with an average width of 45 nm. d) Interconnected nanowires. The average height of the above structures is 2 nm.

The strength of the voltage pulses applied here (15–24 V range) is relatively small; however, the associated fields are quite large, ~3–10 V nm^{-1}, because tip and sample are very close, ~5–10 nm. Furthermore, the field could be significantly enhanced owing to the presence of nanometer-sized asperities at the end of the tip. This implies that the external energy is high enough to activate the diffusion of the relevant chemical species to initiate and sustain the chemical reaction.

ADVANCED MATERIALS

The presence of four different chemical elements in the nanocell (C, O, H, and Si) gives some uncertainty over the chemical composition of the structures formed. Similarities with AFM nano-oxidation experiments would suggest the formation of a silicon oxide.[22] However, exposure of the nanostructures to HF vapor did not remove them, which indicates the absence of silicon oxide. To determine quantitatively the chemical composition we have performed photoemission spectromicroscopy experiments in a synchrotron radiation facility.[23] A series of rectangular structures of several micrometers in size were generated. AFM images of those structures reveal two major rectangles surrounded by smaller structures, all of them fabricated under the same conditions (Fig. 3a). The height of the structure varies from 6 nm at the edges to 14 nm at the center. Photoemission microscopy images of those structures are shown in Figure 3b. To record them, the electron analyzer was tuned to the kinetic energy of the C 1s core-level orbital. The lighter regions (more emission from C 1s orbitals) match the position of the AFM-fabricated structures while the darker regions correspond to the silicon surface. This image was taken with a spatial resolution of about 200 nm (pixel size).

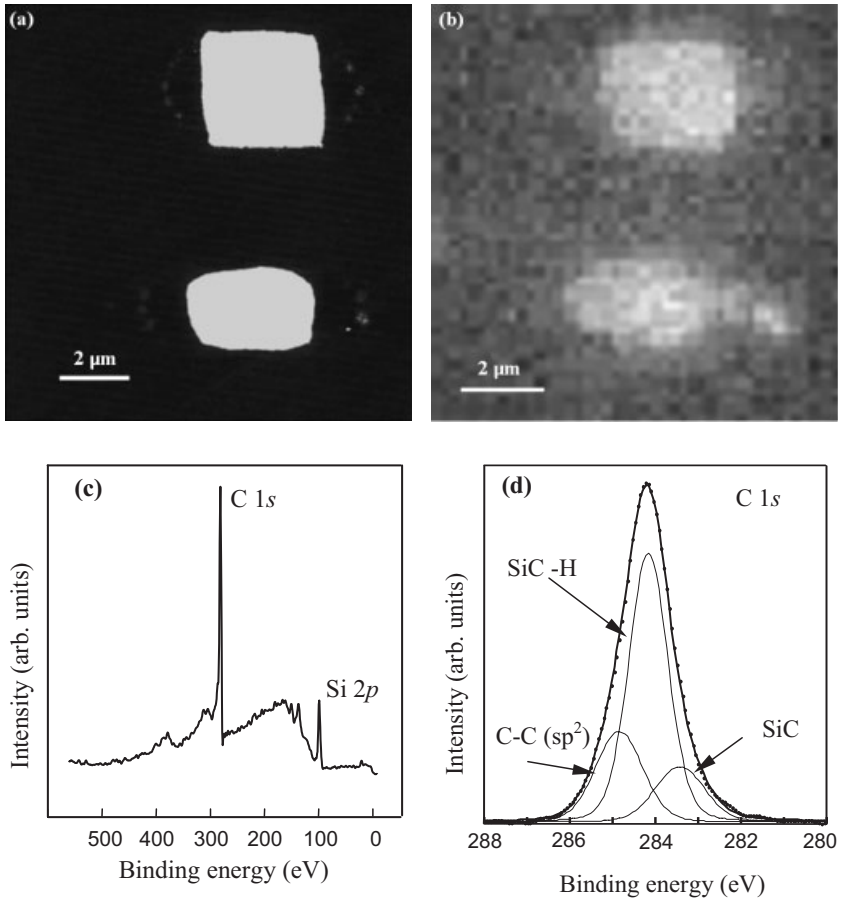

Figure 3. Topographic and spectroscopic images of the fabricated structures. a) AFM image of two rectangular structures. The height of each structure varies from 6 nm at the edges to 14 nm at the center. b) X-ray photoemission spectroscopy (XPS) image of the fabricated structures taken at the energy of the C 1s core level. c) XPS spectrum recorded in the middle of the upper rectangle. Similar spectra were obtained in the other points of upper and lower rectangles. d) C 1s core-level photoemission spectrum of a nanostructure. The three deconvolutions are also plotted. The thick solid line represents the fit, and the points the experimental data.

The XPS spectra recorded on the center of the upper structure reveals two well-defined peaks (Fig. 3c). The higher signal is centered at the C 1s core-level binding energy (~284 eV) while the smaller peak corresponds to the emission from the Si 2p core level (~101 eV). The other minor features in the spectra are easily associated with other core levels or multiple-electron excitations.[24] A higher-resolution spectrum on the C 1s emission shows the peak is centered at 284.2 eV (Fig. 3d). The experimental data points were fitted and deconvoluted into three components, which are shown together with the best fit obtained. In the deconvolution process, Lorenztian and Gaussian widths of 190 meV and 1 eV, respectively, were used. The binding energies of the components are 284.8, 284.1, and 283.4 eV. Those components can be assigned to C–C sp^2 orbitals such as those in graphite, hydrogenated SiC[25] (Si_3C–H environment), and SiC,[26,27] respectively. The formation of SiC and the incorporation of hydrogen in the compound is also supported by the study of the core-level-shifted components of the Si 2p photoemission peak (not shown). The broad and symmetric peak at 2.3 eV-higher binding energies than the Si 2p peak in bulk silicon corresponds to the SiC energy.[25–27] Furthermore, we have performed some in-situ measurements of some reference samples during the same experimental run. For instance, C 1s emission from a highly oriented pyrolitic graphite sample was measured and found to give a sharp peak at 284.8 eV.

In Figure 3d the intensity ratio C/Si deviates from the 1:1 stoichiometry towards a C-rich SiC/H (2.5:1) stoichiometry. This could be a result of either a C-rich surface termination or a substitution of some Si atoms by H. The presence of oxygen in the structures has been disregarded because of the low intensity of the oxygen O 1s peak. Furthermore, the presence of oxygen in SiC gives components at 104–106 eV[28] which have not been observed in these experiments.

The overall chemical reaction leading to the formation of a carbon-rich SiC could be as follows:

$$\mathrm{Si} + x/2\,\mathrm{CH_3{-}CH_2OH} \rightarrow \mathrm{SiC}_x + x\mathrm{H_2} + x/2\,\mathrm{H_2O} \quad (1)$$

where the variable x reflects the non-stoichiometric character of the formed SiC compound.

Silicon carbide is a wide-bandgap semiconductor with good thermal conductivity and high electrical breakdown field.[29] The nanolithographic process developed here allows the fabrication of carbon-rich silicon carbide structures that in combination with silicon oxide barriers could allow the development of high-performance nanometer-sized transistors and sensors.

In summary, we have demonstrated a process for the fabrication of ordered low-dimensional structures of SiC_x on Si substrates. The process is based on the field-induced formation of nanometer-sized ethyl alcohol menisci between a sharp conductive surface and a silicon surface. This is accomplished by using a dynamic AFM operating in a chamber exposed to ethyl alcohol vapor. Meniscus size and kinetic parameters control the nanostructure size. The method yields dots or wires, the width of which ranges from few tens up to a few hundred nanometers. These low-dimensional structures are fabricated at predetermined positions on the substrate. The accuracy of the nanolithographic process allows the fabrication of arrays of nanowires placed 70 nm apart and with diameters below 45 nm. The process is fully compatible with macroscopic processing so the precise chemical composition of the nanostructures can be determined. Finally, we would like to emphasize that this process opens a general method for the bottom–up fabrication of nanomaterials based on the spatial confinement of a chemical reaction within a nanometer-sized meniscus. Menisci of different liquids can be formed, which would allow the production of a large variety of nanostructure compositions that are easily addressed and positioned and amenable to precise electrical and chemical characterization.

Experimental

Nanofabrication: The experiments were performed with a dynamic AFM operating in the low-amplitude solution (non-contact) mode [30] and with additional circuits to perform the oxidation [6]. The microscope was placed into a closed box with inlets for dry nitrogen and alcohol vapor. First, the chamber was purged of water vapor by flushing it with dry N_2 for about 30 min. This reduced the relative humidity below 2 %. Then, the chamber was filled with ethyl alcohol vapor. Non-contact AFM oxidations were performed with doped n^+-type silicon cantilevers (Nanosensors, Germany). The force constant k_c and resonance frequency f_0 were about 25 N m^{-1} and 280 kHz, respectively. The cantilever was excited at its resonance frequency. The semiconductor samples were p-type Si(100) with resistivities of 0.1–1.4 Ω cm. Because of exposure to air, the sample surface is covered by a native silicon oxide of about 1 nm thickness. The alcohol menisci bridging tip and sample were field-induced by applying an external voltage between tip and sample. The sample (anode) is biased positive with respect to the tip. The protocol is similar to the one previously applied to the field-induced formation of water bridges [6,15].

Spectromicroscopy: The spectromicroscopy measurements reported here were performed with the scanning photoemission microscope of the electron spectroscopy for chemical analysis (ESCA) microscopy beamline at the Elettra Synchrotron Light Source. The photon beam was demagnified to a micro-spot of ~200 nm diameter by means of a Fresnel zone plate and the photoelectrons produced were collected by a hemispherical electron energy analyzer with a multi-channel detector. A detailed description of the microscope and associated facilities has been reported elsewhere [23]. Two-dimensional maps of the sample surface were obtained by scanning the sample with respect to the focused X-ray beam and collecting the photoelectrons with a selected kinetic energy at each scan step. Spectra were acquired from small regions with the X-ray micro-spot dimensions. The electron take-off angle was 30° to the sample surface, which enhanced the surface contribution in the data collected. A photon energy of 645 eV was used for all the photoemission measurements with an overall energy resolution of ~220 meV.

Received: September 7, 2004
Final version: March 10, 2005

[1] *Alternative Lithography: Unleashing the Potential of Nanotechnology* (Ed: C. M. Sotomayor Torres), Kluwer Academic/Plenum Publishers, New York **2003**.
[2] G. Binnig, H. Rohrer, *Rev. Mod. Phys.* **1999**, *71*, S324.
[3] C. F. Quate, *Surf. Sci.* **1997**, *386*, 259.
[4] J. A. Dagata, *Science* **1995**, *270*, 1625.
[5] G. Binnig, M. Despont, U. Drechsler, W. Häberle, M. Lutwyche, P. Vettiger, H. J. Mamin, B. W. Chui, T. W. Kenny, *Appl. Phys. Lett.* **1999**, *74*, 1329.
[6] R. Garcia, M. Calleja, H. Rohrer, *J. Appl. Phys.* **1999**, *86*, 1898.
[7] E. B. Cooper, S. R. Manalis, H. Fang, H. Dai, K. Matsumoto, S. C. Minne, T. Hunt, C. F. Quate, *Appl. Phys. Lett.* **1999**, *75*, 3566.
[8] A. Fuhrer, S. Lüscher, T. Ihn, T. Heinzel, K. Ensslin, W. Wegscheider, M. Bichler, *Nature* **2001**, *413*, 822.
[9] V. Bouchiat, M. Faucher, C. Thirion, W. Wernsdorfer, T. Fournier, B. Pannetier, *Appl. Phys. Lett.* **2001**, *79*, 123.
[10] R. Garcia, M. Tello, J. F. Moulin, F. Biscarini, *Nano Lett.* **2004**, *4*, 1115.
[11] S. Hoeppener, R. Maoz, J. Sagiv, *Nano Lett.* **2003**, *3*, 761.
[12] M. Cavallini, P. Mei, F. Biscarini, R. Garcia, *Appl. Phys. Lett.* **2003**, *83*, 5286.
[13] H. Sugimura, N. Nakagiri, *Jpn. J. Appl. Phys.* **1995**, *34*, 3406.
[14] S. Gomez-Moñivas, J. J. Saenz, M. Calleja, R. Garcia, *Phys. Rev. Lett.* **2003**, *91*, 56 101.
[15] M. Calleja, M. Tello, R. Garcia, *J. Appl. Phys.* **2002**, *92*, 5539.
[16] E. S. Snow, P. M. Campbell, R. W. Rendell, F. A. Buot, D. Park, C. R. K. Marian, R. Magno, *Appl. Phys. Lett.* **1998**, *72*, 3071.
[17] X. N. Xie, H. J. Chung, C. H. Sow, A. T. S. Wee, *Appl. Phys. Lett.* **2004**, *84*, 4914.
[18] T. Yoshinobu, J. Suzuki, H. Kurooka, W. C. Moon, H. Iwasaki, *Electrochim. Acta* **2003**, *48*, 3131.
[19] F. S. S. Chien, Y. C. Chou, T. T. Chen, W.-F. Hsieh, T.-S. Chao, S. Gwo, *Appl. Phys. Lett.* **1999**, *75*, 2429.
[20] R. Maoz, E. Frydman, S. R. Cohen, J. Sagiv, *Adv. Mater.* **2000**, *12*, 725.
[21] M. Tello, R. Garcia, *Appl. Phys. Lett.* **2003**, *83*, 2339.
[22] M. Lazzarino, S. Heun, B. Ressel, K. C. Prince, P. Pingue, C. Ascoli, *Appl. Phys. Lett.* **2002**, *81*, 2842.
[23] M. Marsi, M. Casalis, L. Gregoratti, S. Gunther, A. Kolmakov, J. Kovac, D. Lonza, M. Kiskinova, *J. Electron Spectrosc. Relat. Phenom.* **1997**, *84*, 73.
[24] D. P. Woodruff, T. A. Dolcher, *Modern Techniques of Surface Science*, Cambridge University Press, Cambridge, UK **1994**.
[25] C. Virojonandra, L. I. Johansson, *Phys. Rev. B* **2003**, *68*, 125 314.
[26] Y. Hoshino, T. Nishimura, T. Yoneda, K. Ogawa, H. Namba, Y. Kido, *Surf. Sci.* **2002**, *505*, 234.
[27] N. Sieber, T. Seyller, L. Ley, D. James, J. D. Riley, R. C. G. Leckey, M. Polcik, *Phys. Rev. B* **2003**, *67*, 205 304.
[28] F. Amy, P. Soukiassian, Y. K. Hwu, C. Brylinski, *Phys. Rev. B* **2002** *65*, 165 323.
[29] P. G. Neudeck, *J. Electron. Mater.* **1995**, *24*, 283.
[30] R. Garcia, A. San Paulo, *Phys. Rev. B* **1999**, *60*, 4961.

